Carbohydrate Research 346 (2011) 285–293

Contents lists available at ScienceDirect

Carbohydrate Research

journal homepage: www.elsevier.com/locate/carres

Controlled transformation from nanorods to vesicles induced by cyclomaltoheptaoses (β-cyclodextrins)

Tao Sun [a], Huacheng Zhang [a], Li Kong [a], Hongwei Qiao [b], Yueming Li [a], Feifei Xin [a], Aiyou Hao [a,*]

[a] School of Chemistry and Chemical Engineering and Key Laboratory of Colloid and Interface Chemistry of Ministry of Education, Shandong University, Jinan 250100, PR China
[b] Shandong Shengquan Chemical Co., Ltd, Jinan 250204, PR China

ARTICLE INFO

Article history:
Received 27 July 2010
Received in revised form 27 October 2010
Accepted 1 November 2010
Available online 5 November 2010

Keywords:
Cyclodextrin
Anthraquinone
Nanorods
Vesicles
Inclusion complex
Responsive

ABSTRACT

A modified cyclomaltoheptaose (β-cyclodextrin) containing an anthraquinone moiety, mono[6-deoxy-*N*-*n*-hexylamino-(*N*′-1-anthraquinone)]-β-cyclodextrin (**1**), which can self-assemble into nanorods in aqueous solution, was synthesized. Interestingly, upon the addition of natural cyclodextrin, the nanorods could transform into bilayer vesicles, which were characterized by transmission electron microscopy (TEM), scanning electron microscopy (SEM), dynamic light scattering (DLS), and epi-fluorescence microscopy (EFM). A transformation mechanism is suggested based on the results of ^{1}H NMR, 2D NMR ROESY, FTIR, and UV–vis spectra. The response of the vesicles to changing pH and adding Cu^{2+} was also tested. Our research may pave the way to the development of new intelligent materials and biomaterials.

1. Introduction

Self-assembled nanostructures, which have easily-controlled and responsive morphologies,[1–3] are of great interest for their widespread application in molecular machines,[4] biomimicry,[5] and delivery of drugs or genes.[6–8] Supramolecular materials can be tailored from specifically designed molecular components through self-assembly and self-organization that are programmed under the control of directional noncovalent interactions. Nanostructures based on cyclodextrin would combine the properties of molecular devices and macrocyclic host molecules together.[1–3] Cyclomaltooligosaccharides (cyclodextrins, CDs), a class of cyclic oligosaccharides with six to eight D-glucose units linked by α-(1→4)-glucose bonds, have been extensively investigated in molecular recognition and construction of versatile supramolecular architectures.[9] More promising applications are possible if the cyclodextrin cavities can function as independent host sites for molecular recognition when they are confined to the nanostructure. The recognition process is also a useful model of the ligands and receptors on the surface of cell membranes.[10]

Herein, a modified cyclomaltoheptaose (β-cyclodextrin) containing an anthraquinone moiety, mono[6-deoxy-*N*-*n*-hexylamino-(*N*′-1-anthraquinone)]-β-cyclodextrin (**1**), as a fluorescent and functional cyclodextrin derivative, was synthesized (Scheme 1). From TEM (transmission electron microscopy) observations, **1** was able to form nanorods in aqueous solution due to π-stacking of the anthraquinone groups and hydrogen bonding between the cyclodextrins. When natural β-cyclodextrin was introduced into the system, the nanorods were found to transform into vesicles, because of the formation of special amphiphiles by the inclusion of the anthraquinone moiety in the natural β-cyclodextrin, which disrupted the π–π stacking of the nanorods. Cyclodextrins in both nanorods and vesicles can function as independent host sites. Furthermore, the vesicles were responsive to external stimuli, such as pH and added Cu^{2+}.

We regard supramolecular materials as promising materials to meet the requirement for well-defined, regular, directional, and multi-responsive nanoarchitectures, which can be applied in areas, such as biomaterials, drug delivery materials, molecular devices, and intelligent materials.

2. Results and discussion

2.1. Synthesis and characterization

Mono [6-(2-aminohexylamino)-6-deoxy]-β-cyclodextrin (**2**) was prepared according to the literature.[11,12] Complex **1** was prepared by the reaction of **2** and 1-nitroanthraquinone (Scheme 1).

To rule out the possibility of a competitive host–guest complexation reaction typical of cyclodextrins, the host–guest complex of mono [6-(2-aminohexylamino)-6-deoxy]-β-cyclodextrin with

* Corresponding author. Tel.: +86 531 88363306; fax: +86 531 88564464.
E-mail address: haoay@sdu.edu.cn (A. Hao).

0008-6215/$ - see front matter © 2010 Elsevier Ltd. All rights reserved.
doi:10.1016/j.carres.2010.11.003

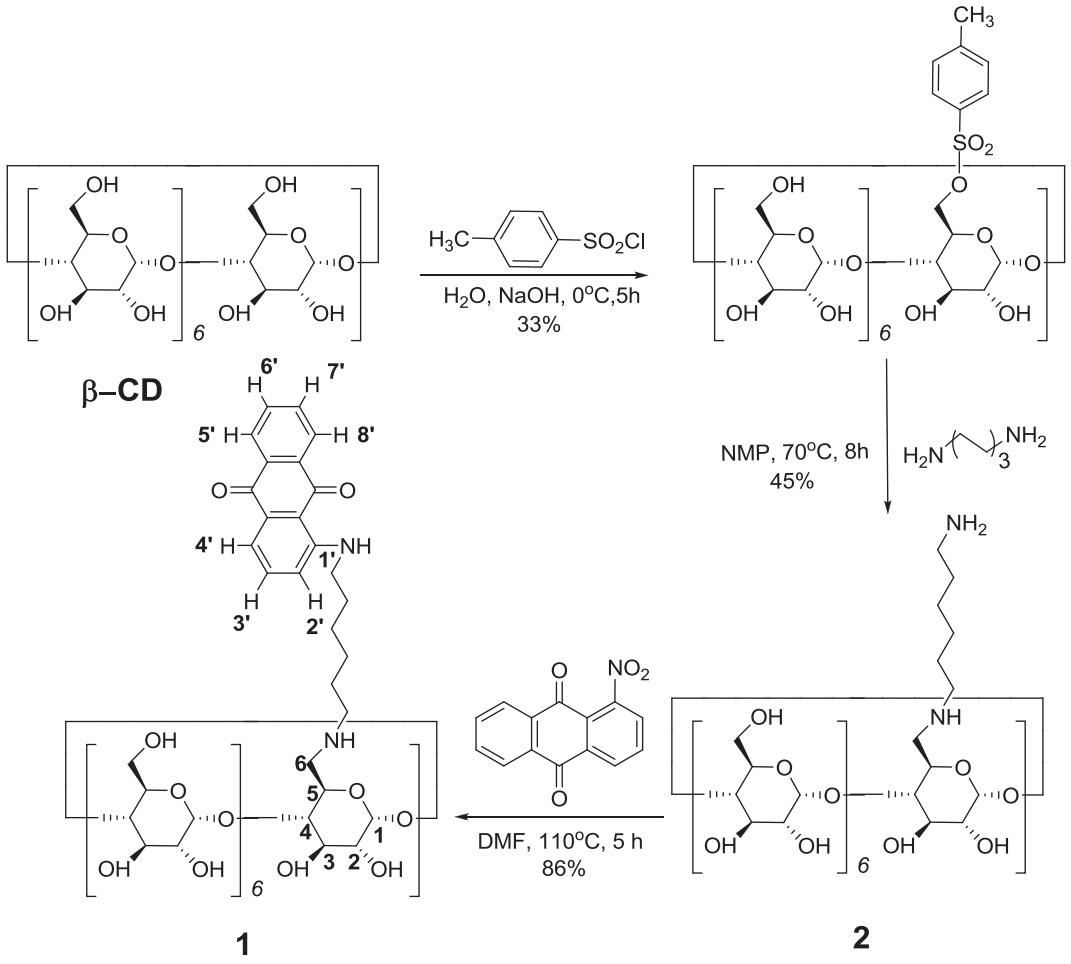

Scheme 1.

1-aminoanthraquinone (**3**) was also prepared. There were typical distinguishing patterns in the TLC, MS, FTIR, and X-ray diffraction (XRD) data between the inclusion complex and the covalently bonded CD-anthraquinone **1** (see Supplementary data).

A benefit of grafting anthraquinone onto cyclodextrin is that the nanorod building block **1** is moderately water soluble. In this work, the water solubility of **1** was measured to be as much as 16 mg/mL (25 °C). It should be emphasized that **1** has similar water solubility to that of β-CD, which is potentially advantageous for its application in biological systems. The surface tension value (60.67 mN m^{-1}, 10^{-4} mol/L, 25 °C) is lower than that of pure water (72 mN m^{-1}, 25 °C), which shows that **1,** as a conjugate of a hydrophilic β-CD with a hydrophobic anthraquinone, is surface active.

2.2. Morphologies

TEM and SEM, which are reliable methods for studying micro-aggregates[13,27,28], were employed to investigate the nanostructures of the nanorods and vesicles formed by **1** in aqueous solution. The aggregation behavior of **1** with a concentration of 10^{-4} mol/L in aqueous solution and the morphology of the obtained supramolecular assembly are reflected in both the TEM and SEM images (Fig. 1a and b). The images show a well-ordered 1D nano-rod structure about 500 nm in width and 5 μm in length. The nanorods are stable for up to two weeks at 300 K in water. The well-defined nanorods may be useful in building smart materials and in solid-state fluorescence sensing.[10]

Upon the introduction of an equimolar amount of natural cyclodextrin, the nanorods can transform into bilayer vesicles, which were characterized by TEM, SEM, DLS, and EFM. Fig. 1c shows clear and monodisperse spherical micro-aggregates with vesicular shells. The particles show a strong contrast between the center and the periphery, which is a characteristic typical of vesicular structures.[27,28] It also can be observed that the vesicles are formed of multi-layers (see Supplementary data). The diameters ranged approximately from 200 to 300 nm. The DLS results (Fig. 2) show that the particles are spherical, with diameters ranging from 50 nm to 300 nm, which is slightly smaller than that found by TEM.[28] The discrepancy seems reasonable because TEM and DLS show solid and swollen vesicles, respectively. SEM and EFM (Fig. 1d and e) were also performed for further confirmation of the vesicles' structures. Because they were sputter-coated with gold to enhance the electrical conductivity, the SEM images show round outlines of collapsed vesicles, and the swollen structures can be clearly observed. From the color contrast of the SEM images, hollow cavities with diameters ranging approximately from 100 to 300 nm were observed, which is consistent with the results of TEM and DLS. In general, TEM, SEM, and DLS are in good agreement in the size-measure. Microspheres with strong fluorescence were observed by EFM. Several drops of a solution of **1** on a glass slide were observed under the fluorescence microscope and microspheres with strong fluorescence were clearly observed and found to undergo a typical Brownian movement. A study on the Brownian movement of nanoparticles could prove useful in the analysis of the gel–vesicle transformation process.[14] It is clear that spherical structures were formed and dispersed homogeneously in the solution. Because of the limited amplification of EFM (100×), the bilayer could not be clearly distinguished.[15,16] Notably, when the

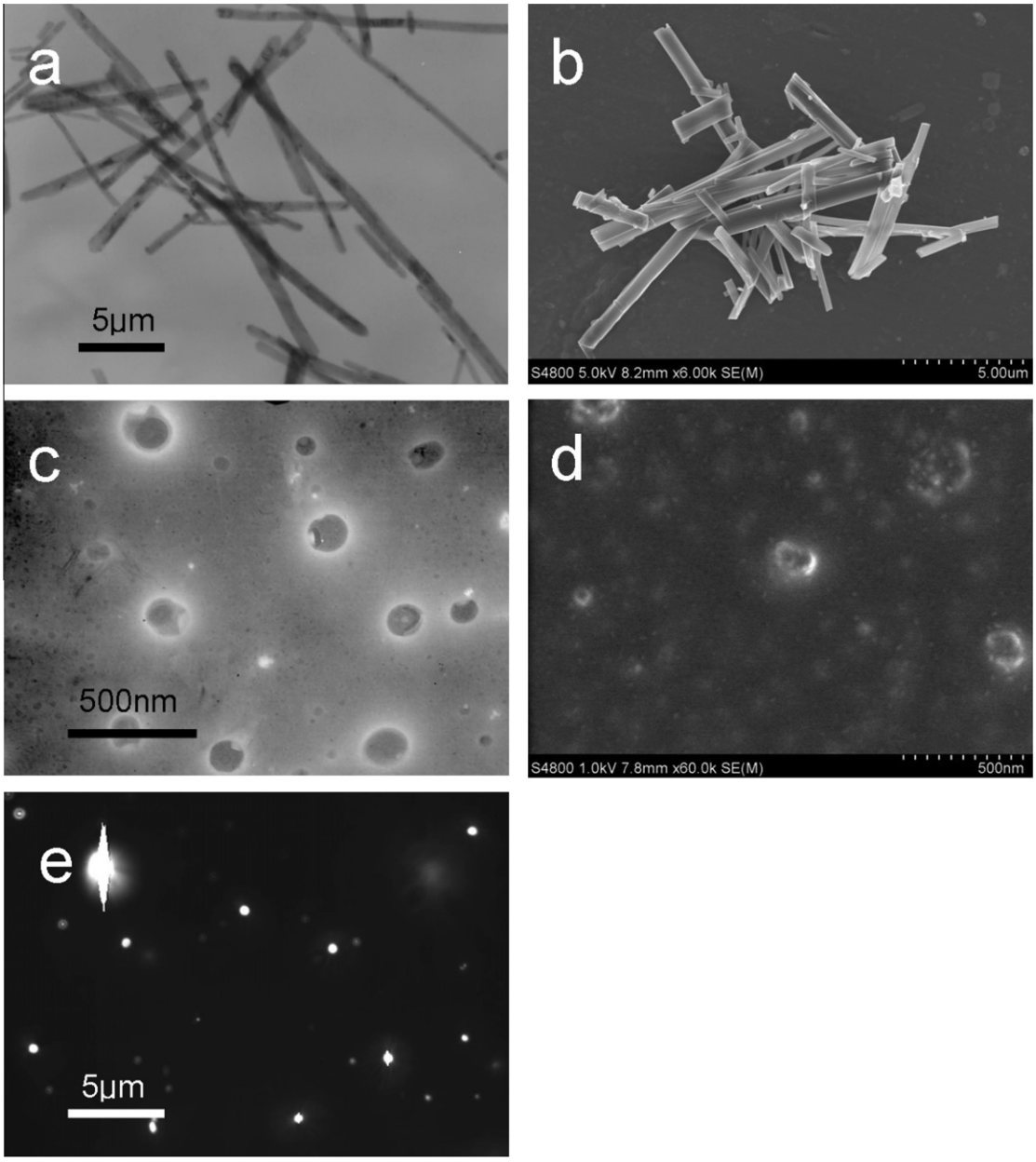

Figure 1. (a) TEM images of the nanorods formed by **1**, with phosphotungstic acid as the negative staining agent; (b) SEM images of the nanorods formed by **1**; (c) TEM images of vesicles formed by **1** and β-CD, with phosphotungstic acid as the negative staining agent; (d) SEM images of vesicles formed by **1** and β-CD; (e) EFM images of vesicles formed by **1** and β-CD, ×100.

image was amplified 100 times, cross features in the vesicle solution were detected for the first time (Fig. 1e). This unusual result may arise from an interference pattern because of the different fluorescence intensities between the inner and outer surfaces of the vesicles.

2.3. The possible mechanism

Similarly to other reported π systems with solubilizing substituents[17,10], **1** is capable of π–π aggregation in aqueous solution. Since **1** is moderately soluble in water, the π–π stacking behavior of **1** could be investigated in aqueous solution. The most direct and dependable evidence for the transformation behavior from nanorods to vesicles was obtained using ^{1}H NMR, 2D NMR ROESY, FTIR, and UV–vis spectroscopy.

The UV–vis spectra of **1** in different solutions further demonstrates the π–π stacking phenomenon. In aqueous solution, **1** shows a small but significant broadening of the peak from 450 to 600 nm in the absorption spectra compared with the spectra in organic solvents (Fig. 3). The π–π stacking behavior can be indicated based on the vibrational shoulder in the absorption spectra in water. Enhancement with respect to the 0–0 transition for the transition from the ground state to the higher electronic states (0–1, 0–2, and 0–3) is shown by the broadening of a vibrational shoulder.[10,22] The differences among the absorption intensities may be due to the variable solubility of the π–π stacked aggregates in different solutions.

The anthraquinone moiety is a well-known component of dyestuffs because of their delocalized conjugated π system. Anthraquinone compounds very easily form the self-assembly by π–π stacking. It is established that there is a competition between inclusion and π–π stacking. However, it seems that under such a low concentration, **1** is inclined to exist in π–π stacking instead of an inclusion complex because π–π stacking interplay is perhaps

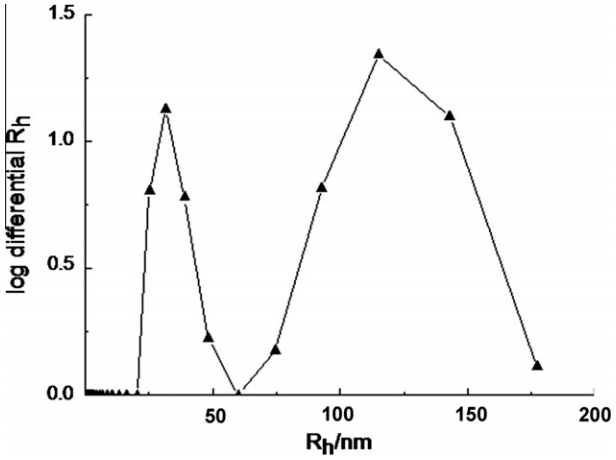

Figure 2. DLS of the vesicles assembled from **1**/β-CD in aqueous solution (1.0×10^{-4} mol/L) at room temperature.

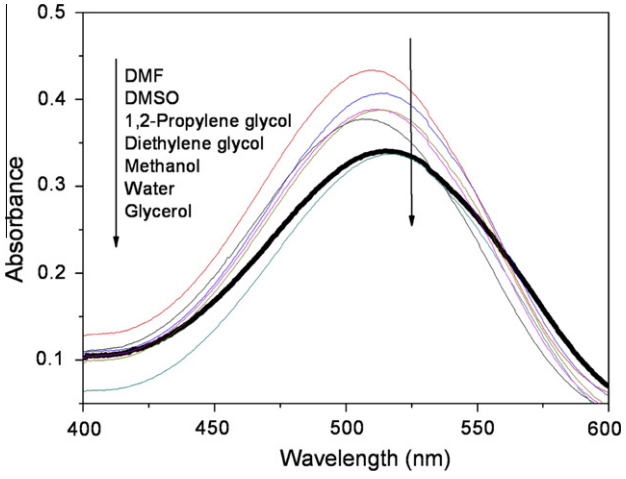

Figure 3. UV–vis spectra of **1** (1.0×10^{-4} mol/L) in different solvents at 25 °C.

stronger than the hydrophobic–hydrophobic interactions. Meanwhile, hydrogen bonding between face-to-face cyclodextrin moieties also plays a very important role in the self-assembly process. If there is no hydrogen bonding between the cyclodextrin moieties, and the inclusion phenomenon is based only on the π–π stacking, the cyclodextrin moieties would be free like 'waving flags'. As a result of the dual binding of the building blocks, the nanorods can be so regular and well-defined.

The UV–vis spectra of **1** of different concentrations changed when an equimolar amount of β-CD was added into the aqueous solution (Fig. 4). It was found that upon the introduction of natural β-CD, the UV–vis absorbance peak (about 515 nm) of **1** is stronger. According to the literature reports[25,26], these small but significant changes in the absorption spectra suggest that there is an interaction between the anthraquinone moiety of **1** and the added β-CD. The change of the UV–vis spectra was attributed to the induction of high electron density in the added β-CD cavity, which suggested that the anthraquinone moiety of **1** would enter the cavity of the added β-CD to form a supramolecular inclusion complex.[23–26]

The spatial conformations and interaction between the molecules can be characterized by 2D ROESY NMR spectroscopy, which has a maximal observation limit within a spatial proximity of 5 Å.[18–21] The ROESY spectra were taken in the absence and the presence of β-CD. A selected region of the ROESY (600 MHz) spectrum of **1** with a concentration of 10^{-4} mol/L in D_2O is shown in Fig. 5. The peaks at 8.01, 7.80, 7.55, and 7.23 ppm belong to H-7′, H-8′, H-3′, and H-2′ on the substituted anthraquinone rings, respectively. Correlations between the hydrogen atoms of H-2′/H-3′, H-7′/H-2′, and H-7′/H-8′ can be clearly observed, which demonstrates the interactions between anthraquinone moieties belonging to different molecules as well as π–π stacking behavior. The correlation between H-2′ and H-3′ is very strong, which demonstrates that the π–π stacking of the anthraquinone moieties is face-to-face in the same direction, which may be due to the hydrogen bond involving the imino group. Strong correlations between the face-to-face cyclodextrin moieties are also found, which means the presence of hydrogen bonding. No hydrogen correlations between anthraquinone and cyclodextrin moieties were found (The full 2D NMR ROESY spectra can be seen in the Supplementary data). The ROESY results mentioned above indicate that the π–π stacking and the hydrogen bonding between face-to-face cyclodextrin moieties are the main driving force in the formation of the nanorods. The nanorods are regular and well-defined, which are similar to the previously reported 'two head' perylene bisimide with two β-CD grafts.[10]

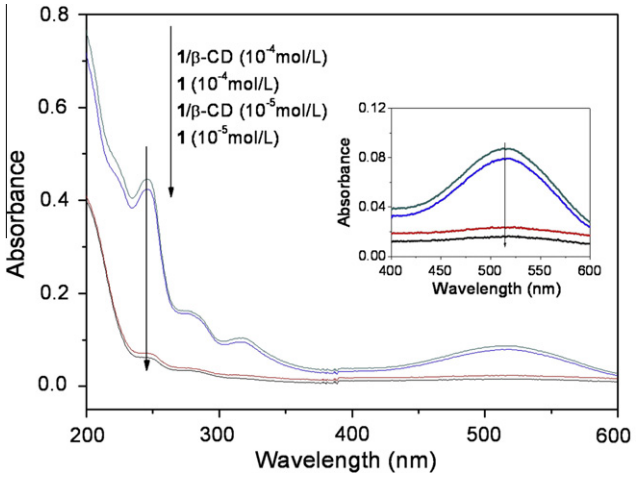

Figure 4. UV spectra of **1** (1.0×10^{-5} mol/L, blue line), **1**/β-CD (1.0×10^{-5} mol/L, red line), **1** (1.0×10^{-4} mol/L, black line) and **1**/β-CD (1.0×10^{-4} mol/L, green line). T = 300 K. (For interpretation of the references to colour in this figure legend, the reader is referred to the web version of this article.)

The selected region of the ROESY (600 MHz) spectrum of **1**/β-CD sample in D_2O with a concentration of 10^{-4} mol/L is shown in Figure 6. The chemical shifts ranging from 3.7 to 3.9 ppm correspond to H-3 to H-6, belonging to natural β-CD or **1**. Upon adding equivalents of β-CD to an aqueous solution of **1**, correlations between H-2′/H-3′and the hydrogens of cyclodextrins can be clearly observed. These correlations could not be detected in a solution of **1** alone. Though the chemical shifts (from 3.7 to 3.9 ppm) of cyclodextrin and **1** cannot be distinguished, the comparison of the correlations between **1** and **1**/β-CD can demonstrate that the anthraquinone moieties on **1** are recognized by the cavity of the added β-CD to form the inclusion complex. The ROESY spectrum revealed an unsymmetrical conformation of the guest molecule inside the cavity, which may be due to the strong hydrogen bonds between anthraquinone moiety and β-CD upon complexation. The inclusion result is also in accordance with that reported in the literature.[37]

^{1}H NMR spectroscopy is one of the most powerful tools for analyzing supramolecular assemblies in solution. Clear chemical shifts of the ^{1}H NMR peaks of **1** were observed corresponding to protons on the anthraquinone moieties in the absence and the presence of β-CD. According to the data, we could judge that β-CD and **1**

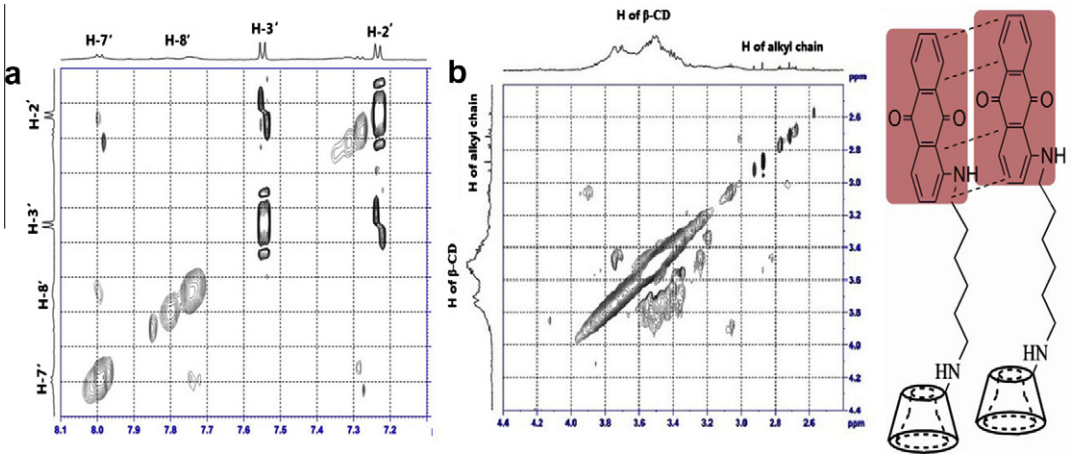

Figure 5. Selected regions of 2D NMR ROESY (600 MHz) spectrum of **1** (1.0×10^{-4} mol/L) in D_2O at ambient temperature, (a) correlation between the anthraquinone moieties; (b) correlations between the cyclodextrin moieties.

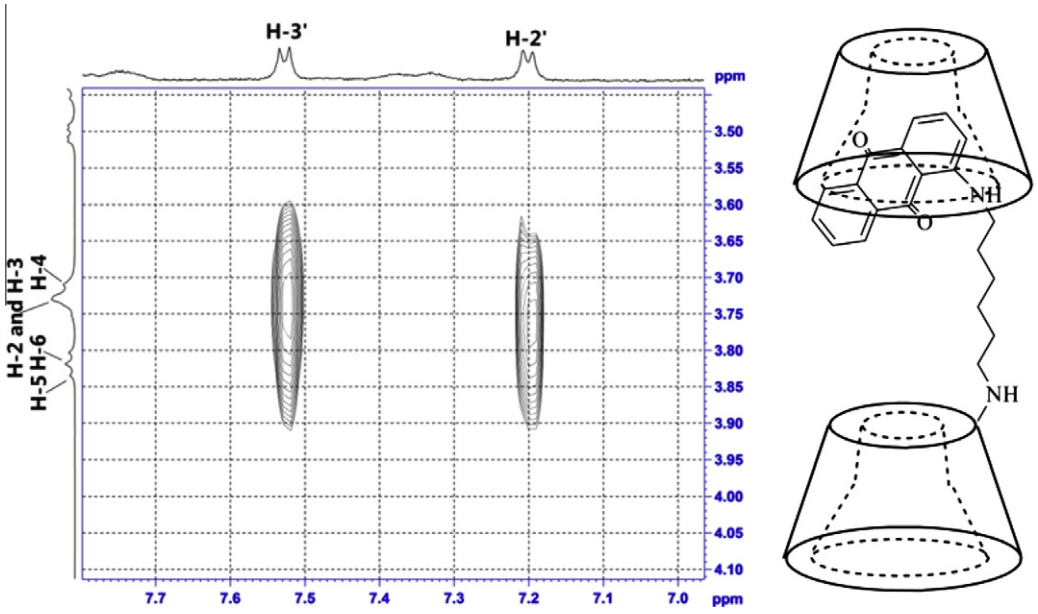

Figure 6. Selected regions of 2D NMR ROESY (600 MHz) spectrum of **1**/β-CD (1.0×10^{-4} mol/L) in D_2O at ambient temperature.

combined. In the presence of natural β-CD, almost all the hydrogen resonances of the anthraquinone moieties of **1** showed chemical shifts (Table 1). Large downfield shifts were observed for H-2′ (7.238→7.201), H-3′ (7.550→7.525), H-7′ (7.795→7.798), and H-8′ (7.779→7.781). From the comparison, it is clear that the substituted ring of anthraquinone entered the β-CD cavity from the secondary side.

The spatial conformation of the inclusion complex can be further confirmed by FTIR spectroscopy, which is a useful method for studying supramolecular inclusion complexes.[27,28] A comparison of the FTIR spectra of the solid inclusion of **1**/β-CD and the physical mixture of **1**/β-CD was also undertaken (Fig. 7). In the physical mixture, the stretching vibration of the hydroxyl group appears in the region of 3391.6 cm^{-1}, while in the solid inclusion complex the peak shifts to 3406.6 cm^{-1} and becomes much wider, which indicates formation of hydrogen bonds between **1** and β-CD. The characteristic absorption band of C=O in the physical mixture, which appeared in the region of 1635.3 cm^{-1}, changed greatly both in peak form and intensity. The differences between the physical mixture and the inclusion complex indicate that the anthraquinone moiety of **1** was included into the cavity of added natural β-CD to form the inclusion complex.[27,28]

A primary criterion for the inclusion of a guest molecule within the host's cavity is obviously its size, and then other factors, such as a strict fit, Van der Waals' interactions, hydrogen bonding, and so on are also important. Anthraquinone has been reported to bind in the β-CD cavity. One possible inclusion structure of the anthraquinone moiety in the β-CD with a cavity opening size of 6.5 Å is an unsymmetrical conformation, due to the size of the

Table 1
The chemical shifts of ^1H NMR from H-1 to H-6

Entry	H-2′	H-3′	H-7′	H-8′
δ (**1**)[a]	7.238	7.550	7.795	7.779
δ (**1**/β-CD)[b]	7.201	7.525	7.798	7.781
Δδ[c]	0.037	0.025	−0.003	−0.002

[a] All the samples were measured in a solution of D_2O, $T = 300$ K.
[b] The complex of 1/β-CD was measured with a concenteation of 10^{-4} mol/L in order to coincide with the concentration of vesicle-formation.
[c] $\Delta\delta = \delta$ (**1**) − δ (**1**/β-CD).

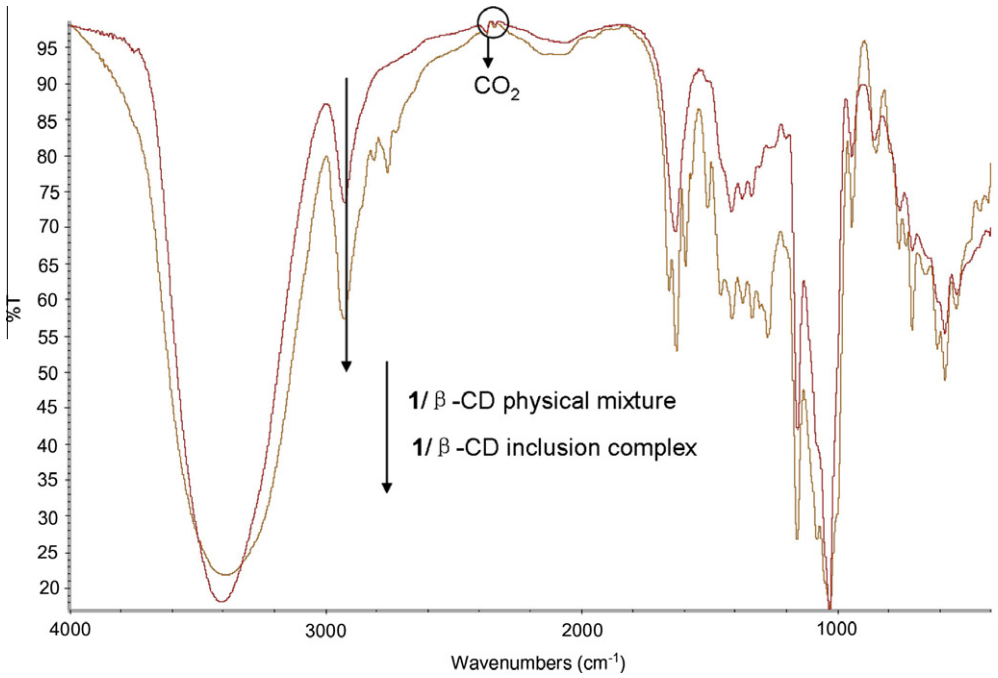

Figure 7. FTIR spectra of the **1**/β-CD inclusion complex (orange line) and **1**/β-CD physical mixture (red line). The peaks from CO_2 (2336 cm^{-1} and 2362 cm^{-1}) are indicated in the figure as the interior label. (For interpretation of the references to colour in this figure legend, the reader is referred to the web version of this article.)

guest molecules in this direction. However, the inclusion is supposed to be only partial. In this case, the central ring bearing two C=O groups, as well as the alkyl-substituted aminobenzene ring, will be inside the cavity of the β-CD, participating in H-bonding with the secondary hydroxyl groups of β-CD, while the unsubstituted benzene ring will be outside the cavity of the β-CD (Scheme 2).

Sole **1** exists in aqueous solution as nanorods (Fig. 8a). Upon the addition of 0.2 M amount of β-CD, the surface and shape of the nanorods begin to change, while some nanospheres with a diameter about 50 nm begin to appear (Fig. 8b). When the molar ratio is 1:0.8, only tiny nanorods are left. Many nanospheres are present, and vesicular structures ranging from 150 nm to 250 nm begin to form. It is easy to observe that the vesicles are formed by the assembly of the nanospheres (Fig. 8c). When the molar ratio is 1:1, typical vesicular structures with multi-layers are formed as referred to in our manuscript (Fig. 8d). If we continue to increase the amount of β-CD to 1:1.2, no obvious changes are found except a tiny decrease of the radius of the vesicles (Fig. 8e).

Upon the introduction of natural β-CD and prolonged ultrasonic treatment, the dissociative **1** can bind with the added β-CD to form a more stable non-covalent amphiphile, then self-assemble into vesicular structures. As a shift occurs in the equilibrium, the nanorods gradually transform into vesicles (Eq. 1).

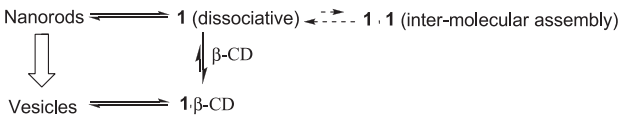

(1)

It should be noted that no vesicles were detected by TEM in aqueous solutions of **1** or β-CD alone. Thus, the combination of **1** and β-CD is crucial for the transformation from nanorods to vesicles. To some extent, the mechanism of vesicle formation herein is similar to the mechanism for the aggregation of non-covalent bola-amphiphiles described in our previous work.[29,30]

2.4. The vesicles' response to pH and Cu^{2+}

TEM experiments showed that the vesicles would disappear upon the addition of equimolar $CuCl_2$ or acetic acid. The shift of the UV peaks of **1** in the presence of Cu^{2+} indicates that **1** can complex with this ion (Fig. 9). It is known that Cu^{2+} easily coordinates with N atoms.[31,32] The vesicles are also responsive to H^+. The UV spectrum, similar to the results after addition of $CuCl_2$, also has a significant variation upon the addition of acetic acid, perhaps because of the change form a secondary amine to a quaternary ammonium species.

Both Cu^{2+} and H^+ hinder the formation of self-assembly aggregates. The reason may be the increase of the electrostatic repulsive force between the 'building blocks', which makes the aggregates difficult to form (Scheme 3). The results described may provide new opportunities in mimicking some biological process. Since it is known that the cancer cells can cause an acidic environment[33–36], H^+-responsive vesicles have potential for building new pH-controlled cancer drug-release systems and pH-responsive materials.

3. Conclusions

In summary, we constructed a supramolecular nanorod aggregate in aqueous solution from the special amphiphile composed of a conjunction of cyclodextrin and anthraquinone **1**. The nanorods transform into vesicles upon the introduction of cyclodextrin, which acts as a dissociation agent for the π–π stacking. The possible mechanisms of the formation of the nanorods and vesicles are suggested based on the results of TEM, SEM, DLS, EFM, UV–vis, and 2D NMR ROESY. The vesicles are responsive to Cu^{2+}/H^+. Understanding the cyclodextrin-linked-anthraquinone system may hopefully provide a sophisticated pathway for the design of intelligent materials with high sensitivity and selectivity. We believe the supramolecular system will also be useful in the fields of biomaterials and cell mimicry.

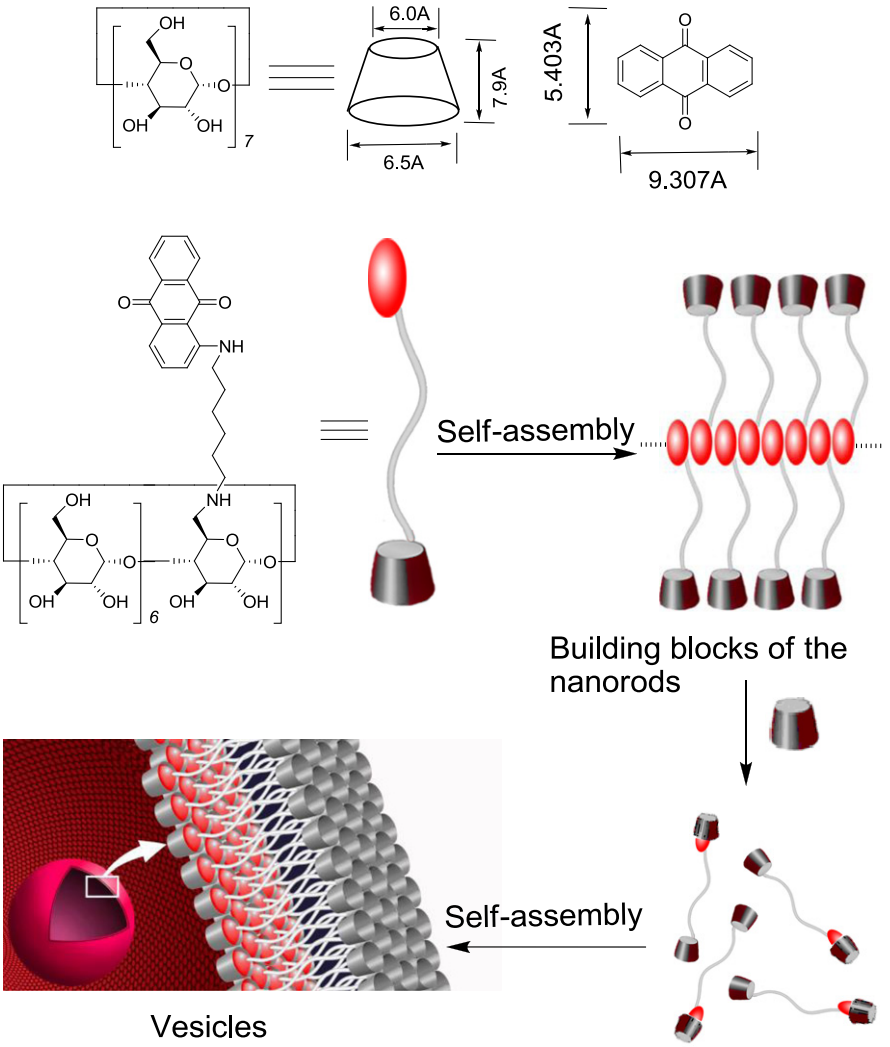

Scheme 2. Illustration of the formation mechanism of the nanorods and vesicles.

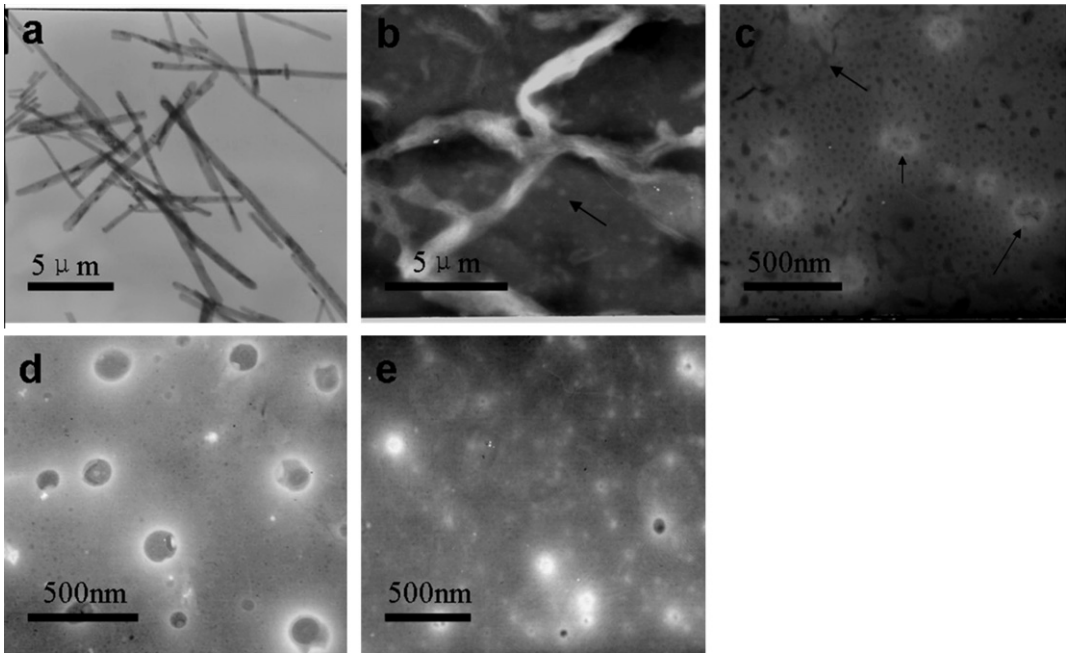

Figure 8. TEM images of the nanostructure formed by 1/β-CD with different molar ratios, with phosphotungstic acid as the negative staining agent; (a) **1**/β-CD = 1:0; (b) **1**/β-CD = 1:0.2; (c) **1**/β-CD = 1:0.8; (d) **1**/β-CD = 1:1; (e) **1**/β-CD = 1:1.2; the concentration of **1** was all set as 10^{-4} mol/L.

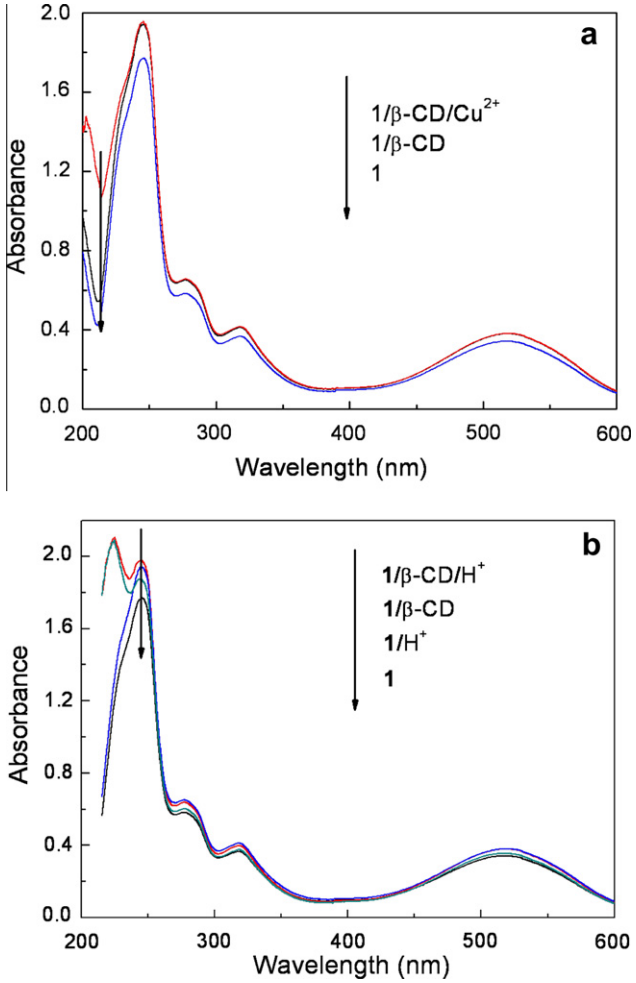

Figure 9. (a) UV spectra of **1** (black line), **1**/β-CD (blue line), the mixture of **1** and acetic acid (green line), the mixture of **1**/β-CD and acetic acid (red line). [**1**] = [**1**/β-CD] = [acetic acid] = 10^{-4}mol/L. T = 300 K. (b) UV spectra of **1** (blue line), **1**/β-CD (black line), the mixture of **1**/β-CD and $CuCl_2$ (red line, solution of [$CuCl_2$] = 10^{-4} mol/L was as the baseline), [**1**] = [**1**/β-CD] = [$CuCl_2$] = 10^{-4} mol/L. T = 300 K. (For interpretation of the references to colour in this figure legend, the reader is referred to the web version of this article.)

4. Experimental

4.1. Materials

1-Nitroanthraquinone was a gift from Shandong Aokete Chemical Reagent Co. Ltd, China. β-CD, recrystallized twice from distilled water and dried in vacuum for 12 h, was purchased from Guangdong Yunan Chemical Reagent Co. Ltd, China. *N,N*-Dimethylformamide (DMF) was firstly dried over $MgSO_4$ for one day and then was distilled in vacuum. Other reagents were all commercially available from Country Medicine Reagent Co. Ltd, Shanghai, China. All other organic reagents were of analytical purity and used as received without further purification. Thin-layer chromatography (TLC) analysis was performed on glass plates precoated with Silica Gel F_{254} obtained from Qingdao Haiyang Chem., China. The developer was a mixture of 2-propanol, water, and aqueous ammonia (30%) (5:2:1, by volume).

4.2. Analytical measurements and methods

^{1}H NMR and ^{13}C NMR spectra were carried out on an API Bruker Avance 400 M NMR at room temperature (rt) with D_2O as the solution and TMS as the reference. 2D ^{1}H–^{1}H ROESY experiments were recorded using an INOVA-600 (600 MHz) spectrometer at ambient temperature. A mixing time of 0.200 s, a relaxation delay time of 1.000 s, and an acquisition time of 0.228 s were used. All pulse sequences were set according to the manufacturer's standards. FTIR spectra were obtained as solutions on an Avatar 370 FTIR spectrometer. All samples for TEM were prepared by the phosphotungstic acid staining technique. The JEM-100CX electron microscope was employed. SEM images were obtained with a Hitachi S-4800 scanning electron microscope by coating the vesicular solution to the base plate, drying, and then sputter-coating with gold. DLS measurements were carried out with a Wyatt Qels Technology Dawn Heleos instrument set at constant room temperature (25 °C) by using a 12-angle replaced detector in a scintillation vial and a 50 mW solid-state laser (λ = 658.0 nm). All solutions for DLS were filtered through a 0.45-μm filter before detection. UV–vis spectra were recorded at room temperature with a TU-1800pc UV–vis spectrophotometer. EFM imaging was performed with an Olympus IX81 fluorescence microscope (Tokyo, Japan) equipped with high-numerical-aperture 60 × (1.45 NA) and 100 × (1.40 NA) oil-immersion objective lens, a mercury lamp source, a mirror unit consisting of a 330–385 nm excitation filter (BP330-385), a 455 nm dichromatic mirror (DM 455), emission filter (IF510-550), and a 16-bit thermoelectrically cooled EMCCD (Cascade 512B, Tucson, AZ, USA). Imaging acquisition and data analysis were performed using MetaMorph software (Universal Imaging, Downingtown, PA, USA). The XRD experiments were performed on a German Bruker/D8 ADVANCE diffractometer with Cu Kα radiation (λ = 0.15406 nm, 40 kV, 40 mA). The sonication was performed with a KQ116 ultrasonic cleaner, Kunshan ultrasonic apparatus Co. Ltd, China.

4.3. Synthetic route of the cyclodextrin–anthraquinone coupling system 1

Mono[6-(2-aminohexylamino)-6-deoxy]-β-cyclodextrin (**2**) was prepared according to the literature.[11,12] To a solution of DMF (10 mL) containing 2.72 g (2 mmol) of mono[6-(2-aminohexylamino)-6-deoxy]-β-cyclodextrin, 0.61 g (2.4 mmol) of 1-nitroanthraquinone was added. The reaction mixture was stirred for 5 h at 85 °C and monitored by TLC, then cooled and poured into 25 mL of acetone. The mixture was filtered and the cake was washed with acetone three times. The crude product was further purified by silica gel column chromatography with an mixed eluent of 10:2:1 2-propanol–water–30% aq ammonia to give the product **1** (513 mg), in a yield of 18%: rose red powder, R_f 0.6 (with a mixed developer of 5:2:1 2-propanol–water–30% aq ammonia), ^{1}H NMR (600 MHz, D_2O, 300 K, TMS): δ 7.955 (s, 2H, *H*-6′*H*-7′), 7.743 (s, 2H, *H*-5′*H*-8′), 7.759 (d, 1H, *H*-4′), 7.745 (d, 2H, *H*-2′*H*-3′), 4.935 (d, 7.1H, *H*-1), 3.845–3.504 (m, 43.5H, *H*-2 to *H*-6), 1.253–1.157 (m, 12.6H, $(CH_2)_6$). FTIR (KBr plate, ν cm^{-1}): 3404.02 (vs, br, ν_{OH}), 2924.52 (s, ν_{CH2}), 1662.91(m, δ_{NH}), 1031.58 (s, δ_{CH}). ESIMS: calcd for $C_{62}H_{90}N_2O_{36}H^+$ *m/z* 1439.54; found *m/z* 1440.20; calcd for $C_{62}H_{90}N_2O_{36}Na^+$ *m/z* 1461.52; found *m/z* 1461.97. Anal. Calcd for $C_{62}H_{90}N_2O_{36}$: C, 51.74; H, 6.30; N, 1.95. Found: C, 51.81; H, 6.41; N, 1.87.

4.4. Preparation of the nanorods and vesicles

Molar quantified mother solutions of **1**, 1×10^{-3} mol/L, were prepared by adding 0.146 g of **1** into 100 mL of triply distilled water at 300 K. All sample solutions for the nanorod investigation were freshly prepared by diluting the stock solution, followed by sonication for 20 min at 300 K. The sample vesicular solutions were prepared by mixing the same volume of **1** (2×10^{-4} mol/L) and of β-CD (2×10^{-4} mol/L) solutions, with sonication for 20 min at 300 K before detection. The effect of an external stimulus was

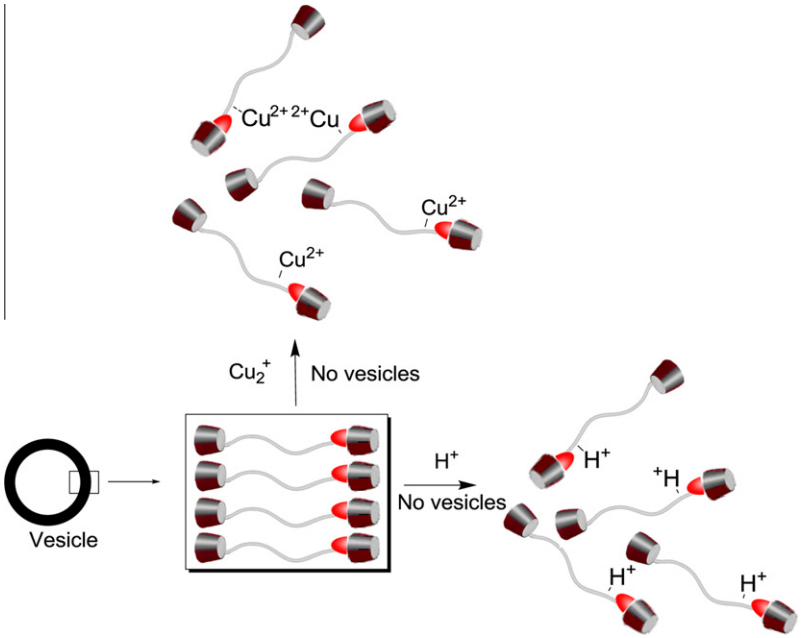

Scheme 3. Illustration of the disappearance of the vesicles upon addition of Cu^{2+} ions and acetic acid.

investigated by adding external substances (acetic acid and Cu^{2+}) to the sample solutions.

4.5. Preparation of the solid inclusion complex and physical mixture of 1 and β-CD

β-CD (1 mmol) was dissolved in water of 60 °C (15 mL) and a clear solution formed. Compound **1** (1 mmol, 0.5 mL) was added slowly and stirred for half an hour then cooled down. The aqueous solution of **1**/β-CD was distilled under reduced pressure at room temperature to remove the water and obtain the solid inclusion complex. In order to make the FTIR comparison, a physical mixture of **1** and β-CD was needed. To make the physical mixture, **1** (1 mmol) and β-CD (1 mmol) were ground with KBr separately, well mixed, and then pelleted in order to avoid the inclusion of guest and host molecule during the grinding procedure.[9]

Acknowledgments

This work was supported by the NSFC (Grant No. 20625307), National Basic Research Program of China (973 Program, 2009CB930103) and Graduate Independent Innovation Foundation of Shandong University (GIIFSDU, yzc09057). The authors thank Dr. Pamela Holt from USA for editing the manuscript and Dr. Z. Yang from Université Pierre et Marie Curie: Paris 6 for the figure adjustment.

Supplementary data

Supplementary data associated with this article can be found, in the online version, at doi:10.1016/j.carres.2010.11.003.

References

1. Sortino, S.; Mazzaglia, A.; Scolaro, L. M.; Merlo, F. M.; Valveri, V.; Sciortino, M. T. *Biomaterials* **2006**, *27*, 4256–4265.
2. Falvey, P.; Lim, C. W.; Darcy, R.; Revermann, T.; Karst, U.; Giesbers, M.; Marcelis, A. T. M.; Lazar, A.; Coleman, A.; Reinhoudt, D.; Ravoo, B. J. *Chem. Eur. J.* **2005**, *11*, 1171–1180.
3. Mazzaglia, A.; Ravoo, B. J.; Gambadauro, R. D. P.; Mallamace, F. *Langmuir* **2002**, *18*, 1945–1948.
4. Akira, H. *Acc. Chem. Res.* **2001**, *34*, 456–464.
5. Okada, S.; Peng, S.; Spevak, W.; Charych, D. *Acc. Chem. Res.* **1998**, *31*, 229–239.
6. Guo, X.; Szoka, F. C. *Acc. Chem. Res.* **2003**, *36*, 335–341.
7. Mazzaglia, A.; Angelini, N.; Lombardo, D.; Micali, N.; Patane, S.; Villari, V.; Scolaro, L. M. *J. Phys. Chem. B* **2005**, *109*, 7258–7265.
8. Allen, T. M.; Cullis, P. R. *Science* **2004**, *303*, 1818–1822.
9. Szejtli, J. *Chem. Rev.* **1998**, *98*, 1743–1754.
10. Liu, Y.; Wang, K. R.; Guo, D. S.; Jiang, B. P. *Adv. Funct. Mater.* **2009**, *19*, 2230–2235.
11. Brady, B.; Lynam, N.; O'Sullivan, T.; Ahern, C.; Darcy, R. *Org. Synth. Collect.* **2004**, *10*, 686; *Org. Synth.* **2000**, *77*, 220–224.
12. Samal, S.; Geckeler, K. E. *Chem. Commun. (Cambridge)* **2001**, 2224–2225.
13. Jing, B.; Chen, X.; Wang, X.; Yang, C.; Xie, Y.; Qiu, H. *Chem. Eur. J.* **2007**, *13*, 9137–9142.
14. Jesorka, A.; Markstrom, M.; Karlsson, M.; Orwar, O. *J. Phys. Chem. B* **2005**, *109*, 14759–14763.
15. Xu, Y.; Wang, G.; Zhao, X.; Jiang, X.; Li, Z. *Langmuir* **2009**, *25*, 2684–2688.
16. Horbaschek, K.; Hoffmann, H.; Thunig, C. *J. Colloid Interf. Sci.* **1998**, *206*, 439–456.
17. Zang, L.; Che, Y.; Moore, J. S. *Acc. Chem. Res.* **2008**, *41*, 1596–1608.
18. Liu, J.; Alvarez, J.; Ong, W.; Roman, E.; Kaifer, A. E. *J. Am. Chem. Soc.* **2001**, *123*, 11148–11154.
19. Liu, W.; Xie, T.; Liang, Y.; Liu, W.; Ma, Y. J. *Organomet. Chem.* **2001**, *627*, 93–98.
20. Skinner, P. J.; Blair, S.; Kataky, R.; Parker, D. *New J. Chem.* **2000**, *24*, 265–268.
21. Han, Y.; Cheng, K.; Simon, K. A.; Lan, Y.; Sejwal, P.; Luk, Y. Y. *J. Am. Chem. Soc.* **2006**, *128*, 13913–13920.
22. Wurthner, F. *Chem. Commun. (Cambridge)* **2004**, 1564–1579.
23. Cramer, F. D. *Pure Appl. Chem.* **2004**, *76*, 1825–1845.
24. Tong, L. H.; Hu, J.; Liu, Y. 13th International Symposium on Macrocyclic Chemistry, Book of Abstracts, Gesellschaft Deutscher Chemiker, Gundlachdruck, Hamberg, 1998, p 120.
25. Cramer, F.; Saenger, W.; Spatz, H. C. *J. Am. Chem. Soc.* **1967**, *89*, 14–20.
26. Tong, L. H. *Cyclodextrin Chemistry—Foundation and Application*; Science Press: Beijing, 2001; p 135.
27. Li, G.; Mcgown, L. B. *Science* **1994**, *264*, 249–251.
28. Maurice, R.; Eftink, M. L.; Bystrom, K.; Perlmutter, H. D.; Kristol, D. S. *J. Am. Chem. Soc.* **1989**, *111*, 6765–6772.
29. Zhang, H.; Shen, J.; Liu, Z.; Bai, Y.; An, W.; Hao, A. *Carbohydr. Res.* **2009**, *344*, 2028–2035.
30. Zhang, H.; An, W.; Liu, Z.; Hao, A.; Hao, J.; Shen, J.; Zhao, X.; Sun, H.; Sun, L. *Carbohydr. Res.* **2009**, *345*, 87–96.
31. Masakatsu, S.; Motomu, K. *Chem. Rev.* **2008**, *108*, 2853–2873.
32. Bernardo, K.; Leppard, S.; Robert, A.; Commenges, G.; Dahan, F.; Meunier, B. *Inorg. Chem.* **1996**, *35*, 387–396.
33. Bhujwalla, Z. M.; Mccoy, C. L.; Glickson, J. D.; Gillies, R. J.; Stubbs, M. *Brit. J. Cancer* **1998**, *78*, 606–611.
34. Beselli, R.; Renzi, G.; Morello, R.; Altieri, F. *J. Craniofac. Surg.* **2007**, *18*, 1051–1054.
35. Yamagata, M.; Tannock, I. F. *Brit. J. Cancer* **1996**, *73*, 1328–1334.
36. Tannock, I. F.; Rotin, D. *Cancer* **1989**, *49*, 4373–4384.
37. Jiang, H.; Sun, H.; Zhang, S.; Hua, R.; Xu, Y.; Jin, S.; Gong, H.; Li, L. *J. Inclusion Phenom. Macro.* **2007**, *58*, 133–138.